

Geodesics in information geometry: Classical and quantum phase transitions

Prashant Kumar,^{*} Subhash Mahapatra,[†] Prabwal Phukon,[‡] and Tapobrata Sarkar[§]*Department of Physics, Indian Institute of Technology, Kanpur 208016, India*

(Received 10 August 2012; published 16 November 2012)

We study geodesics on the parameter manifold for systems exhibiting second order classical and quantum phase transitions. The coupled nonlinear geodesic equations are solved numerically for a variety of models which show such phase transitions in the thermodynamic limit. It is established that both in the classical as well as in the quantum cases, geodesics are confined to a single phase and exhibit turning behavior near critical points. Our results are indicative of a geometric universality in widely different physical systems.

DOI: [10.1103/PhysRevE.86.051117](https://doi.org/10.1103/PhysRevE.86.051117)

PACS number(s): 05.70.Fh, 64.70.Tg

I. INTRODUCTION

Information theoretic studies of phase transitions are, by now, well established. The underlying idea here is geometric in nature and rests on the definition of a Riemannian metric tensor on the space of parameters (called parameter manifold) of a system. Depending on whether the interactions of the system are classical or quantum in nature, this metric might be induced from the equilibrium thermodynamic state space [1] (for a review, see [2]) or from the natural Hilbert space structure of quantum states [3]. For the former, the parameter manifold consists of thermodynamic control parameters such as the pressure, volume, and temperature, while for the latter, this might be thought of as the manifold of coupling constants appearing in the Hamiltonian.

Given such a metric tensor, the parameter manifold can have very different properties depending on whether the system undergoes a second order classical or a quantum phase transition (CPT or QPT). Whereas the hallmark of a CPT is that the scalar curvature arising out of the metric diverges at a second order phase transition (and everywhere on the spinodal curve), this is not the case for second order QPTs where the curvature can remain regular [4]. It is also known that whereas some components of the metric tensor vanish at a second order CPT, as these are related to inverses of thermodynamic response coefficients [2], for QPTs, the situation is reversed, and some of the components of the metric tensor diverge at such a transition, as follows from first order perturbation theory [4] (although this may not be true in some special cases, see [5]).

Although a lot of attention has been paid to the behavior of the metric tensor and its associated scalar curvature in the context of phase transitions, much less is known about geodesics, i.e., paths that minimize the distance between two points on the parameter manifold. In any geometric setup, the behavior of geodesics is an important object to study. Some studies on geodesics have appeared in the context of CPTs [6] and QPTs (specifically, for adiabatic quantum computation) [7,8] in special cases. The purpose of this paper is to complement and generalize these results, and to obtain and

analyze general solutions to the geodesic equations for some model systems that exhibit second order phase transitions.

Here, we study four models in the thermodynamic limit: the van der Waals (vdW) model for fluids, the Curie-Weiss (CW) mean-field model of ferromagnetism, the infinite Ising ferromagnetic chain (all of which exhibit CPTs at finite temperature), and the transverse field XY model that exhibits a QPT at zero temperature. For all these models, the full set of coupled nonlinear geodesic equations in the information geometric context are set up and solved numerically, with appropriate initial conditions. To the best of our knowledge, such an analysis has not been performed before. Our treatment is completely general in nature, and differs significantly from the methods used in [6,8] where the focus was on obtaining specific geodesics between two given points in the parameter manifold. Interestingly, we find that in all the examples that we consider, geodesics exhibit a turning point close to criticality. Further, they are “confined” to a single phase, i.e., for CPTs, geodesics that begin from one of the coexisting phases do not cross over to the other phase, while for QPTs, geodesics do not cross the (second order) phase boundaries. This is indicative of a geometric universality in apparently unrelated physical phenomena.

This paper is organized as follows. In the next section, we first briefly recall some basic facts about information geometry and geodesics. We then proceed to analyze the vdW, the CW, and the infinite Ising ferromagnet as illustrations of CPTs. In Sec. III, we analyze the geodesic structure of QPTs via the transverse field XY spin chain. We end in Sec. IV with our discussions and possible directions for future study.

II. INFORMATION GEOMETRY, GEODESICS, AND CLASSICAL PHASE TRANSITIONS

In the context of equilibrium thermodynamics of classical systems, the formulation of information geometry is mainly due to the work of Ruppeiner [2]. The main idea here is to consider the positive definite Riemannian metric arising out of the Hessian of the entropy density s , and given by a line element

$$d\tau^2 = g_{\mu\nu} dx^\mu dx^\nu = -\frac{1}{k_B} \left(\frac{\partial^2 s}{\partial x^\mu \partial x^\nu} \right). \quad (1)$$

Here, x^μ ($\mu = 1, 2$) denotes the internal energy and the particle number per unit volume and are coordinates on the parameter manifold in the “entropy representation.” k_B is the Boltzmann’s

^{*}kprash@iitk.ac.in[†]subhmaha@iitk.ac.in[‡]prabwal@iitk.ac.in[§]tapo@iitk.ac.in

constant, which we will set to unity in what follows. The line element of Eq. (1) introduces the concept of a distance in the space of equilibrium thermodynamic states via fluctuation theory, i.e., the larger this distance is between two given states, the smaller the probability that these are related by a thermal fluctuation. Various representations (related to each other by Legendre transforms) can be used for this geometric construction (a full list can be found in [2]), and a particularly useful diagonal form of the metric for single component fluids and magnetic systems is

$$d\tau^2 = \frac{1}{T} \left(\frac{\partial s}{\partial T} \right)_\rho dT^2 + \frac{1}{T} \left(\frac{\partial \mu}{\partial \rho} \right)_T d\rho^2, \quad (2)$$

where T is the temperature, ρ the number density, and $\mu = \left(\frac{\partial f}{\partial \rho} \right)_T$, f being the Helmholtz free energy per unit volume. For magnetic systems, we need to consider thermodynamic quantities per unit spin, with the magnetization per unit spin m replacing ρ .

On the other hand, information geometry in quantum mechanical systems, first studied by Provost and Vallee [3], is defined by taking two infinitesimally separated quantum states and constructing the quantity

$$|\psi(\vec{x} + d\vec{x}) - \psi(\vec{x})|^2 = \langle \partial_\mu \psi | \partial_\nu \psi \rangle dx^\mu dx^\nu = \alpha_{\mu\nu} dx^\mu dx^\nu, \quad (3)$$

where x^μ [collectively denoted as \vec{x} in the left-hand side of Eq. (3)] denotes the parameters on which the wave function ψ depends, and ∂_μ is a derivative with respect to x^μ . From the $\alpha_{\mu\nu}$ (which are not gauge invariant), a meaningful gauge-invariant metric tensor can be defined as [3]

$$g_{\mu\nu} = \alpha_{\mu\nu} - \beta_\mu \beta_\nu; \quad \beta_\mu = -i \langle \psi(\vec{x}) | \partial_\mu \psi(\vec{x}) \rangle. \quad (4)$$

Here, $g_{\mu\nu}$ is the metric induced from the natural structure of the Hilbert space of quantum states. The metrics in Eqs. (2) and (4) can be used to predict second order phase transitions in both CPTs [2] and QPTs [4]. We also record here the expression for the scalar curvature arising out of the metric in the special case when the metric is diagonal (with $g \equiv \det g_{\mu\nu}$):

$$R = \frac{1}{\sqrt{g}} \left[\frac{\partial}{\partial x^1} \left(\frac{1}{\sqrt{g}} \frac{\partial g_{22}}{\partial x^1} \right) + \frac{\partial}{\partial x^2} \left(\frac{1}{\sqrt{g}} \frac{\partial g_{11}}{\partial x^2} \right) \right]. \quad (5)$$

Given the information geometry of classical or quantum systems, we wish to study geodesics in the same. Let us briefly recall a few elementary facts about geodesics. For a manifold endowed with a metric with components $g_{\mu\nu}$, a geodesic is a path that extremizes the proper distance (or line element, the infinitesimal form of which is given by $d\tau^2 = g_{\mu\nu} dx^\mu dx^\nu$). This can be cast as a variational problem to determine the extrema of the integral $\int_1^2 \sqrt{g_{\mu\nu} \dot{x}^\mu \dot{x}^\nu} d\lambda$, where the dot denotes a derivative with respect to λ , which is an affine parameter, parametrizing the curve joining two points denoted 1 and 2. Calculus of variations can then be applied with the result that geodesic curves are solutions to the differential equations

$$\ddot{x}^\mu + \Gamma_{\nu\rho}^\mu \dot{x}^\nu \dot{x}^\rho = 0$$

with $\Gamma_{\nu\rho}^\mu = \frac{1}{2} g^{\mu\zeta} \left(\frac{\partial g_{\zeta\nu}}{\partial x^\rho} + \frac{\partial g_{\zeta\rho}}{\partial x^\nu} - \frac{\partial g_{\nu\rho}}{\partial x^\zeta} \right).$ (6)

The above equation can also be obtained by writing a “Lagrangian”

$$\mathcal{L} = \frac{1}{2} (g_{\mu\nu} \dot{x}^\mu \dot{x}^\nu) \quad (7)$$

and using the (derivatives of the) Euler-Lagrange equations that follow. This method often provides valuable insights into the symmetries of the system. We will be interested in studying the solutions of Eq. (6) in the context of CPTs and QPTs. It is well known that a natural affine parameter for geodesic curves is $\lambda = \tau$, and thus it is useful to consider the normalized vector $\dot{x}^\mu = dx^\mu/d\tau$ such that $\dot{x}^\mu \dot{x}_\mu = g_{\mu\nu} \dot{x}^\mu \dot{x}^\nu = 1$.

Equation (6), in general, gives rise to a set of coupled nonlinear differential equations, which might be difficult to solve analytically. We will mostly concentrate on numerical solutions with appropriate boundary conditions. Note that in terms of the normalized vector \dot{x}^μ , we need to specify three boundary conditions in order to solve Eq. (6), with the fourth one being fixed by the normalization condition. Namely, we choose a “starting point,” i.e., an initial value of x^μ , and any one component of \dot{x}^μ . The second component of the derivative is then determined from the fact that \dot{x}^μ is normalized. The reader will note that there is an infinite number of such boundary conditions possible, given any starting point. In most of our analysis, we will choose the derivatives appropriately, so that the geodesics are projected towards the critical point (or the critical line, for the case of QPTs). These will be useful for us to determine the behavior of the geodesics close to criticality. With the given boundary conditions, we wish to determine the most general solutions to Eq. (6) and study geodesics near criticality. This is done by solving for x^μ in terms of the affine parameter τ , and tracing out the geodesic near the critical point, by parametrically plotting the resulting solution, under variation of τ .¹ Let us now illustrate the above discussion with the example of the van der Waals fluid and the Curie-Weiss ferromagnet.

A. van der Waals and Curie-Weiss models

Information geometry of the van der Waals fluid is well established (see, e.g., [9]). We start from the Helmholtz free energy per unit volume [10]

$$f_{\text{vdW}} = -\rho T \ln \left(\frac{e}{\rho} \right) + \rho c_v T \ln \left(\frac{e}{T} \right) - \rho T \ln(1 - b\rho) - a\rho^2, \quad (8)$$

where c_v is the specific heat at constant volume, ρ and T are the number density per molecule of fluid and the temperature, a, b are the coefficients arising in the vdW equation of state, and e is the exponential function. It is convenient to work with the reduced vdW equation of state, and we can substitute $a = 9T_c/8\rho_c$, $b = 1/3\rho_c$, where ρ_c and T_c denote the critical values of the density and the temperature, respectively. Further, the reduced density and temperature are defined by $\rho_r = \rho/\rho_c$, $T_r = T/T_c$. We will set $\rho_c = T_c = 1$ to simplify the algebraic

¹We will also keep in mind that geodesic paths are not unique: an elementary example is that of a 2-sphere, where there are an infinite number of geodesics, i.e., great circles, between two antipodal points.

details, and also choose $c_v = 3/2$, the ideal gas value. The information metric (in terms of the coordinates T_r and ρ_r) is then given, from Eq. (2), by

$$g_{TT} = \frac{3}{2} \frac{\rho_r}{T_r^2}, \quad g_{\rho\rho} = \frac{9[4T_r - \rho_r(\rho_r - 3)^2]}{4\rho_r T_r (\rho_r - 3)^2}. \quad (9)$$

Since we are interested in geodesics close to criticality (for a recent related discussion, see [11]), we now expand the metric up to first order about the critical point $(T_r, \rho_r) = (1, 1)$ [remember we have set $(T_c, \rho_c) = (1, 1)$]. The metric components are then given by the simple expressions

$$g_{TT}^c = 3\rho_r \left(\frac{3}{2} - T_r\right), \quad g_{\rho\rho}^c = \frac{9}{4} (T_r - 1), \quad (10)$$

where the superscript c in Eq. (10) signifies that these expressions are valid close to criticality. The geodesic equations of Eq. (6) turn out to be

$$\begin{aligned} \ddot{T}_r + \frac{\dot{T}_r^2}{2T_r - 3} + \frac{\dot{T}_r \dot{\rho}_r}{\rho_r} + \frac{3\dot{\rho}_r^2}{4\rho_r(2T_r - 3)} &= 0, \\ \ddot{\rho}_r + \frac{\dot{\rho}_r \dot{T}_r}{T_r - 1} + \frac{\dot{T}_r^2(2T_r - 3)}{3(T_r - 1)} &= 0. \end{aligned} \quad (11)$$

We now numerically solve Eq. (11) with three boundary conditions: $(T_r, \rho_r, \dot{\rho}_r) = (1.001, 1.007, -0.92)$, $(1.001, 1.009, -1.2)$, and $(1.0007, 1.011, -2.2)$.² For all the three cases, we solve Eq. (11) for values of the affine parameter between 0 and 0.0025. The solutions for T_r and ρ_r are then parametrically plotted by varying the affine

²The value of \dot{T}_r is fixed from the normalization condition as alluded to before.

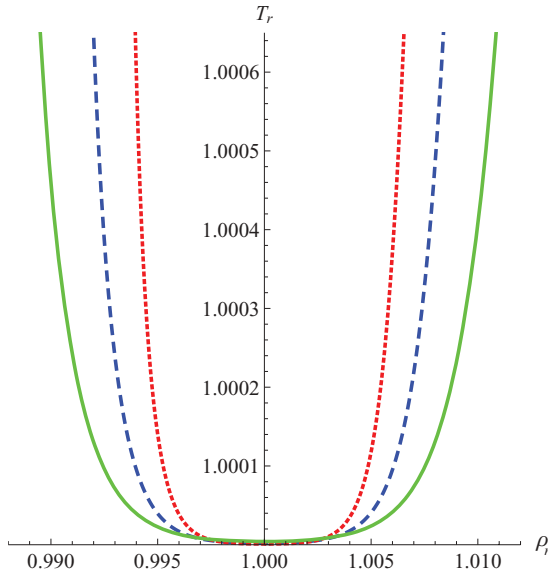


FIG. 1. (Color online) Numerical solution for geodesics of the vdW equation of state close to criticality in the (ρ_r, T_r) plane. The dotted red, dashed blue, and solid green curves correspond to the boundary conditions $(T_r, \rho_r, \dot{\rho}_r) = (1.001, 1.007, -0.92)$, $(1.001, 1.009, -1.2)$, and $(1.0007, 1.011, -2.2)$, respectively. The geodesics turn back from the critical point $(\rho_r, T_r) = (1, 1)$.

parameter. The result is shown in Fig. 1 in the (ρ_r, T_r) plane, where the dotted red, dashed blue, and solid green curves correspond to the three boundary conditions described above, respectively. We see that the geodesic curves “turn back” from the critical point. As we will see, this is a generic feature for all second order phase transitions studied in this paper.

For the sake of completeness, we mention here that the analysis of geodesics using the full vdW metric of Eq. (9) is similar, although the geodesic equations are more complicated and we omit them for brevity. After extensive numerical analysis, our conclusion here is that, as alluded to in the Introduction, a geodesic starting in the liquid ($\rho_r > 1, T_r < 1$) or gas ($\rho_r < 1, T_r < 1$) phase does not reach the other phase. They either terminate at the spinodal line or continue to the supercritical region. This implies that on the parameter manifold, points that lie in different phases are not geodesically connected, and these may be thought of as separated by phase transitions. Such an interpretation also appeared in [6] in the context of the vdW model. Also, close to the critical point, geodesics show the turnaround behavior as depicted in Fig. 1. This is not unexpected since the spinodal curve, being the locus of divergences of the scalar curvature on the parameter manifold, tends to incline the geodesics [6]. We also find that geodesics do not show any special behavior at the binodal lines, i.e., at the location of the first order phase transitions, which is expected because the metric and the scalar curvature are both regular here. These results are summarized in Fig. 2, where we have shown several numerical solutions to the geodesic equations for the vdW equation of state. The dotted green curve is the spinodal curve. The dashed blue curves on the left and the dotted-dashed black curves on the right are geodesics that start from the gas and liquid phases, respectively, and continue into the supercritical region. The solid red curves are geodesics in the supercritical region ($T_r > 1$), and show turning behavior similar to that depicted in Fig. 1.

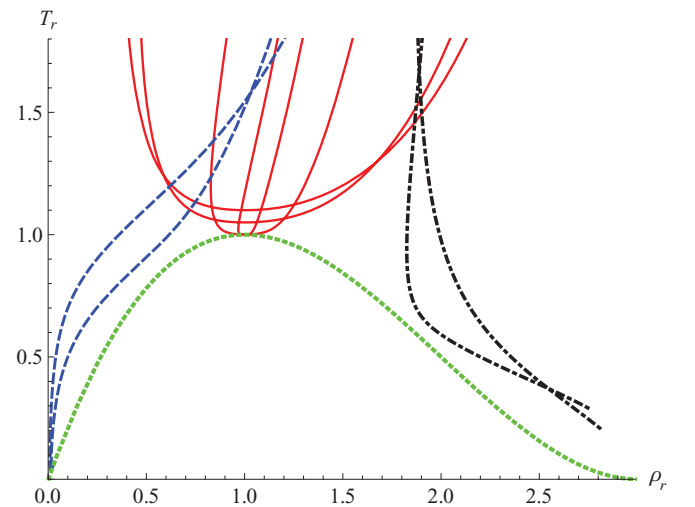


FIG. 2. (Color online) Various numerical solutions for geodesics of the vdW equation of state in the (ρ_r, T_r) plane. The dashed blue, dotted-dashed black, and solid red lines are geodesics that begin from the gas, liquid, and supercritical phases, respectively. The spinodal curve is shown in dotted green.

We now move on to study geodesics in the classical mean-field Curie-Weiss ferromagnetic model in the thermodynamic limit. Information geometry of this model has been studied extensively in [12], and we simply state the result that in the (T, m) representation, the line element of Eq. (2) is given by

$$dl^2 = \frac{C_L}{T^2} dT^2 + \frac{1}{T} \frac{[T_c(1 - m^2) - T]}{m^2 - 1} dm^2. \quad (12)$$

Here, T is the temperature, T_c its critical value, m is the magnetization per unit spin, and $C_L(T)$ is a “lattice specific heat” introduced in [13] that corresponds to the mechanical energy of the lattice. As was shown in [13], information geometry in the CW model can not be defined without introducing this term *ad hoc* in the theory. In [12], it was shown that the line element in Eq. (12) correctly reproduces all the known features of the CW model, including the first order phase transitions. We will study the model close to criticality, and approximate the metric close to $m = 0$ as³

$$g_{TT}^c = \frac{C_L(T)}{T^2}, \quad g_{mm}^c = 1 - \frac{T_c}{T}, \quad (13)$$

where again the superscript c denotes that we are close to criticality. To analyze the geodesic equations here, we note that a crucial simplification is possible since none of the metric components in Eq. (13) depend on the magnetization. This implies that the Lagrangian of Eq. (7) is independent of m , and hence the Euler-Lagrange equation that follows from it implies that $\dot{m} = K/g_{mm}^c$ where K is a constant. Then, from the normalization condition $g_{TT}^c \dot{T}^2 + g_{mm}^c \dot{m}^2 = 1$, it follows that

$$\dot{T}^2 = \frac{1}{g_{TT}^c} \left(1 - \frac{K^2}{g_{mm}^c} \right) = \frac{T^2[T(1 - K^2) - T_c]}{C_L(T)(T - T_c)}. \quad (14)$$

It is enough for us to consider the region $T > T_c$, for which Eq. (14) implies that positivity of the right-hand side imposes the restriction $T > T_c/(1 - K^2)$, with $K^2 < 1$. This means that a geodesic in the region $T > T_c$ always remains in that region and can not cross over into the region $T < T_c$. A pathology arises for the case $K = 0$, for which Eq. (14) implies that such a restriction is not implied since \dot{T}^2 is always a positive number for $K = 0$ or $m = \text{constant}$. We have checked this by explicitly solving the geodesic equations, which in this case are given by

$$\ddot{T} + \frac{\dot{T}^2(T\dot{C}_L - 2C_L)}{2TC_L} - \frac{T_c\dot{m}^2}{2TC_L} = 0, \quad \ddot{m} + \frac{T_c\dot{m}\dot{T}}{T(T - T_c)} = 0. \quad (15)$$

Numerical analyses [after choosing an appropriate regular functional form for $C_L(T)$, such as a power series] reveal that geodesics with $m = \text{constant}$ lines [these are indeed geodesics as they satisfy the second equation in Eq. (15)] cross over inside the spinodal region. This is probably a mathematical artifact and we do not have a physical explanation for this. Apart from these constant m lines, the behavior of geodesics close to the critical point is, as expected, qualitatively similar to

that of the vdW fluid and, graphically, they resemble the ones shown in Fig. 1. We also find that the behavior of geodesics with the full CW metric (away from criticality) is qualitatively similar to those of the vdW model. Specifically, geodesics in the phase $m > 0$ do not reach the phase $m < 0$, and vice versa.

B. Infinite Ising ferromagnet

We now study geodesics in the infinite-range ferromagnetic Ising model with a transverse magnetic field. This model (the Lipkin-Meshkov-Glick model) was studied recently in [14], where it was shown that in the thermodynamic limit, it can be described by the classical dynamics of a single large spin. The information geometric aspects of this model have not been studied so far, and we begin with a discussion on this. The Hamiltonian for this model is given by [14,15] (see [16] for a finite temperature analysis of this model from an entanglement point of view)

$$H_{\text{IF}} = -\frac{J}{N} \sum_{i < j} S_i^z S_j^z - h \sum_i S_i^x = -\frac{J}{2N} (S_{\text{tot}}^z)^2 - h S_{\text{tot}}^x, \quad (16)$$

where the second equality follows from defining the total spin $S_{\text{tot}}^z = \sum_i S_i^z$, $S_{\text{tot}}^x = \sum_i S_i^x$ (and neglecting a constant term). We will set $J = 1$ in what follows. In a mean-field approach, where the average magnetization $m = \sum_i \langle S_i^z \rangle / N$, the Hamiltonian for a single spin reduces to $H_{\text{IF}}^1 = -m S_{\text{tot}}^z - h S_{\text{tot}}^x$. This is an effective two-state model, the partition function of which can be shown to be given by

$$Z = 2 \cosh\left(\frac{\sqrt{h^2 + m^2}}{2T}\right). \quad (17)$$

To understand the geometric aspects of this model, we write the Gibbs free energy for the single spin $G = -T \ln Z$ and effect a Legendre transform to obtain the Helmholtz free energy $F = G + m^2/2$, where m should be thought of as the applied magnetic field, i.e., an intensive thermodynamic variable. The factor of 1/2 in the Legendre transform might look strange, but note that this enforces the magnetization $\partial F / \partial m = 0$ (via the relation $m = -\partial G / \partial m$), i.e., defines the boundary between the ferromagnetic and paramagnetic regions. In (T, m) coordinates, using the expression for the Helmholtz free energy, the metric components are given from Eq. (2) by

$$g_{TT} = \frac{1}{4T^4} (h^2 + m^2) \text{sech}^2 \alpha, \quad (18)$$

$$g_{mm} = \frac{1}{T} - \frac{1}{4T^2} \text{sech}^2 \alpha \frac{[m^2 \sqrt{h^2 + m^2} + h^2 T \sinh(2\alpha)]}{(h^2 + m^2)^{3/2}},$$

where $\alpha = \sqrt{h^2 + m^2}/2T$. The scalar curvature of Eq. (5) for the metric of Eq. (18), in the limit $m \rightarrow 0$ (which is our region of interest), is given by $R = \mathcal{A}/\mathcal{B}$, where

$$\mathcal{A} = h \left[-2T(4h^2 + 4T + 1) \sinh\left(\frac{h}{T}\right) + 4(h^2 + 2T) \tanh\left(\frac{h}{2T}\right) + 3h \text{sech}^2\left(\frac{h}{2T}\right) \right]$$

³This is simpler than expanding the metric about $m = 0$ and $T = T_c$, which gives results equivalent to what we present here.

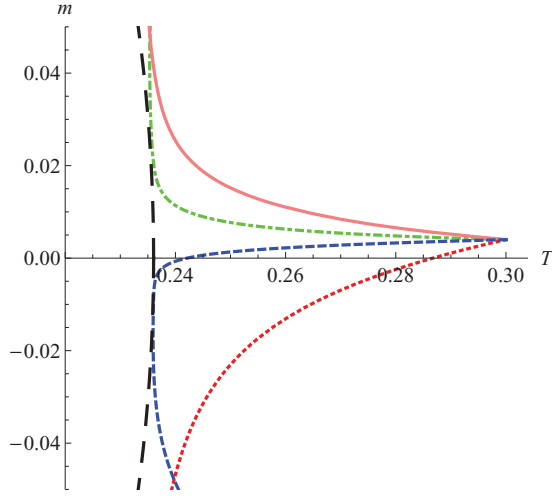


FIG. 3. (Color online) Numerical solution for geodesics of the infinite-range Ising ferromagnet at $h = 0.2$, near the critical point ($T = 0.236, m = 0$). All geodesics are chosen to pass through the point $(T, m) = (0.3, 0.004)$. The dashed blue (small dashes), dotted-dashed green, dotted red, and solid pink curves correspond to the boundary condition $m = -0.03, 0.03, -0.25$, and 0.12 , respectively. The dashed black line on the extreme left (long dashes) is the spinodal curve, on which the scalar curvature diverges.

$$\begin{aligned} & -2T^2 + 2h^2[4T(T-2) - 1] \\ & + 2T[4h^2(T+1) + T]\cosh\left(\frac{h}{T}\right), \\ \mathcal{B} = 2h^2 \left[\tanh\left(\frac{h}{2T}\right) - 2h \right]^2. \end{aligned} \quad (19)$$

The scalar curvature diverges at $\tanh\frac{h}{2T} = 2h$, defining the phase boundary, a result that matches with that obtained in [14]. To understand the behavior of geodesics in this model, we set $h = 0.2$, which implies the critical temperature $T = 0.236$. Numerical solutions of this geodesic equation close to the critical point are plotted in Fig. 3. Here, we have taken all the geodesics to start from $(T, m) = (0.3, 0.004)$. The dashed blue (small dashes), dotted-dashed green, dotted red, and solid pink curves correspond to $m = -0.03, 0.03, -0.25$, and 0.12 , respectively. Also shown in dashed black (long dashes) is the spinodal curve on the extreme left, i.e., the locus of divergence of the scalar curvature arising out of the metric of Eq. (18). We find that the geodesics show the same turning behavior as in the other mean-field models discussed in the previous section. We also note that in the limit of $T \rightarrow 0$, g_{mm} diverges and $g_{TT} \rightarrow 0$. Numerical solutions seem to become somewhat unreliable in this limit, and we will not discuss them.

Having elucidated the nature of geodesics in classical systems exhibiting phase transitions at nonzero temperatures, we finally move to quantum phase transitions at zero temperatures.

III. GEODESICS IN QPTs: THE TRANSVERSE XY SPIN CHAIN

Information geometry of QPTs has been well studied of late, starting from the work of [4]. There are, however, very few systems to which this can be meaningfully applied since

the definition of the geometry [from Eq. (4)] requires complete knowledge of the many body ground state, which may be difficult to obtain excepting for a few exactly solvable systems, such as the transverse field XY spin chain. Even when such ground states are obtainable, as in the Dicke model of quantum optics, explicit calculations might be prohibitively difficult due to algebraic complications. We will base our calculations on the transverse XY model, for which the information metric was obtained in [4].

To recall, for the transverse XY spin chain, the Hamiltonian with $(2N + 1)$ spins is

$$H_{XY} = - \left[\sum_{j=-N}^N \frac{1+\gamma}{4} \sigma_j^x \sigma_{j+1}^x + \frac{1-\gamma}{4} \sigma_j^y \sigma_{j+1}^y - \frac{h}{2} \sigma_j^z \right], \quad (20)$$

where the σ^i , $i = x, y, z$, are Pauli matrices, γ is an anisotropy parameter, h is the magnetic field, and the Planck's constant has been set to unity. The information metric for this model has been calculated in [4] and in the thermodynamic limit, the line element in the region $|h| < 1$, $\gamma > 0$ (the ferromagnetic phase) is given by

$$ds^2 = \frac{dh^2}{16\gamma(1-h^2)} + \frac{d\gamma^2}{16\gamma(1+\gamma)^2}. \quad (21)$$

QPTs occur on the lines $\gamma = 0$, $|h| \leq 1$ (the anisotropic transition line), and $|h| = 1$ (the Ising transition lines), where the spectrum of the theory becomes gapless. Information geometry is, however, very different for these two transitions. Whereas the scalar curvature [calculated from Eqs. (5) and (21)] diverges on the line $\gamma = 0$, it is regular on the lines $|h| = \pm 1$. For this model, the geodesic equations are

$$\ddot{h} + \frac{h\dot{h}^2}{1-h^2} - \frac{\dot{h}\dot{\gamma}}{\gamma} = 0, \quad \ddot{\gamma} - \frac{\dot{\gamma}^2(1+3\gamma)}{2\gamma(1+\gamma)} + \frac{\dot{h}^2(1+\gamma)^2}{2\gamma(1-h^2)} = 0, \quad (22)$$

where, as before, the overdot represents a derivative with respect to the affine parameter τ . Also, the normalization condition implies that

$$\frac{\dot{h}^2}{16\gamma(1-h^2)} + \frac{\dot{\gamma}^2}{16\gamma(1+\gamma)^2} = 1. \quad (23)$$

Before attempting to solve the coupled nonlinear equations of Eq. (22), let us look at a special case. The first of Eq. (22) is satisfied by h as constant and, hence, constant h lines are geodesics. To find γ as a function of the affine parameter in this case, we substitute $\dot{h} = 0$ in the second of Eqs. (22) and (23). Then, it is seen that $\gamma = \tan^2[2(\tau - \tau_0)]$, where τ_0 is a reference value for the affine parameter. Thus, for the constant h geodesics, γ is always positive, i.e., these geodesics do not cross the phase boundary at $\gamma = 0$. Rather, they turn back on touching that line. This should be contrasted with the $m = \text{constant}$ geodesics of the CW model, which, as we have said, is not fully understood.

To solve the equations in Eq. (22) in general, we adopt a numerical procedure analogous to what we have done before. As an illustration, we solve for these equations with the initial conditions $(h, \gamma, \dot{h}) = (0.96, 0.1, -0.0857)$. The solution,

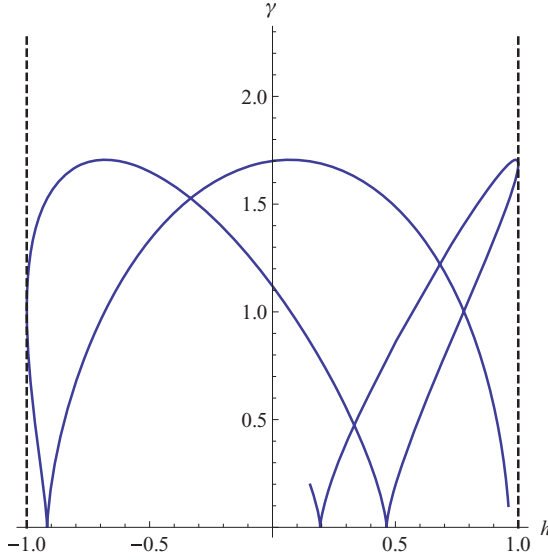


FIG. 4. (Color online) Numerical solution for a geodesic curve with $(h, \gamma) = (0.96, 0.1)$ and $(\dot{h}, \dot{\gamma}) = (-0.0857, 1.35)$ on the h - γ plane. The geodesic (solid blue line) is confined to a single phase region between $h = \pm 1$, shown by the dashed black vertical lines.

plotted on the h - γ plane parametrically, with the affine parameter τ , is shown in Fig. 4. Clearly, the geodesic is confined to a single phase and does not cross the phase boundaries, as in CPTs. It is not difficult to check this analytically by expanding the metric near the lines $\gamma = 0$ and $h = \pm 1$. As mentioned, in contrast to CPTs, the phase boundaries at $h = \pm 1$ do not represent singularities in the scalar curvature of the parameter manifold, which is finite at (but discontinuous across) these lines [4]. The turning behavior of the geodesics here can be traced to the fact that some of the metric components diverge at $h = \pm 1$.

IV. CONCLUSIONS AND DISCUSSIONS

In this paper, we have studied four model systems that exhibit phase transitions in the thermodynamic limit. The

van der Waals model, the Curie-Weiss mean-field model of ferromagnetism, and the infinite Ising ferromagnet exhibit CPTs at finite temperature. The transverse XY spin chain shows a QPT at zero temperature. For all these models, we performed the most general analysis of geodesics in the parameter manifold. Such an analysis has not appeared in the literature before. In the process, we have established the information geometry of the infinite Ising ferromagnet. We have solved the geodesic equations for all these models in full generality by choosing a starting point (i.e., coordinates) in the manifold, and imposing initial conditions on its derivatives with respect to the affine parameter. In this way, we are able to trace out the geodesics and study their behavior near second order critical points. This complements and extends the results of [6,7] in a nontrivial way.

Our main conclusion here is that purely from a geometric perspective, geodesics near critical points show universal behavior, although the physical nature of the phase transitions is widely different. We have also established that geodesics are confined to a single phase: for example, in the classical van der Waals model, a geodesic beginning from one of the coexisting phases does not cross over to the other phase. Similarly, for QPTs, geodesics do not cross the phase boundaries. We believe that these results are model independent, and should be true for any model of CPTs or QPTs.

It might be interesting to study geodesics in the context of scaled equations of state for classical fluid systems, and also for some other models that exhibit QPTs (see, e.g. [17]). In particular, in the context of CPTs, it is an interesting question to ask if geodesics show any special behavior at or near the Widom line, which is a continuation of the coexistence curve, along which the correlation length maximizes. We leave such a study for the future.

ACKNOWLEDGMENTS

It is a pleasure to thank D. Sen for very useful correspondence. The work of S.M. is supported by Grant No. 09/092(0792)-2011-EMR-1 from CSIR, India.

-
- [1] G. Ruppeiner, *Phys. Rev. A* **20**, 1608 (1979).
 - [2] G. Ruppeiner, *Rev. Mod. Phys.* **67**, 605 (1995); **68**, 313 (1996).
 - [3] J. P. Provost and G. Vallee, *Commun. Math. Phys.* **76**, 289 (1980).
 - [4] P. Zanardi, P. Giorda, and M. Cozzini, *Phys. Rev. Lett.* **99**, 100603 (2007).
 - [5] L. Campos Venuti and P. Zanardi, *Phys. Rev. Lett.* **99**, 095701 (2007).
 - [6] L. Diósi, B. Lukács, and A. Rácz, *J. Chem. Phys.* **91**, 3061 (1989).
 - [7] A. T. Rezakhani, W.-J. Kuo, A. Hamma, D. A. Lidar, and P. Zanardi, *Phys. Rev. Lett.* **103**, 080502 (2009).
 - [8] A. T. Rezakhani, D. F. Abasto, D. A. Lidar, and P. Zanardi, *Phys. Rev. A* **82**, 012321 (2010).
 - [9] D. C. Brody and D. W. Hook, *J. Phys. A: Math. Theor.* **42**, 023001 (2008).
 - [10] L. D. Landau and E. M. Lifshitz, *Statistical Physics*, Part 1, Vol. 5 (Elsevier, Amsterdam, 2010).
 - [11] H. Quevedo and A. Ramirez, [arXiv:1205.3544](https://arxiv.org/abs/1205.3544).
 - [12] A. Dey, P. Roy, and T. Sarkar, [arXiv:1111.6721](https://arxiv.org/abs/1111.6721).
 - [13] H. Janyszek and R. Mrugała, *Phys. Rev. A* **39**, 6515 (1989).
 - [14] A. Das, K. Sengupta, D. Sen, and B. K. Chakrabarti, *Phys. Rev. B* **74**, 144423 (2006).
 - [15] A. Dutta, U. Divakaran, D. Sen, B. K. Chakrabarti, T. F. Rosenbaum, and G. Aeppli, [arXiv:1012.0653](https://arxiv.org/abs/1012.0653).
 - [16] J. Wilms, J. Vidal, F. Verstraete, and S. Dusuel, *J. Stat. Mech.* **(2012)** P01023.
 - [17] M. Filippone, S. Dusuel and J. Vidal, *Phys. Rev. A* **83**, 022327 (2011).